SCUOLA DI INGEGNERIA INDUSTRIALE
E DELL'INFORMAZIONE

Executive Summary of the Thesis

Eclipse-Free Station-Keeping for Quasi-Halo Orbits with Application to the LUMIO Mission

Laurea Magistrale in Space Engineering - Ingegneria Spaziale

Author: Giovanni Dalone

Advisor: Dr. Carmine Giordano

Co-advisors: Prof. Francesco Topputo, Alessandro Martinelli

Academic year: 2025-2026

1. Introduction

CubeSats have rapidly evolved into capable platforms for scientific and technological missions beyond Low Earth Orbit. Advances in miniaturized avionics, propulsion, and communication systems now enable deep-space and cislunar operations, as demonstrated by missions such as MarCO and CAPSTONE. However, the intrinsic size constraints of CubeSat platforms impose strict limitations on power generation, battery capacity, and propellant storage, making long-term operations in multi-body environments particularly demanding.

In the cislunar regime, Halo orbits around the collinear libration points of the Earth–Moon system provide favorable geometrical conditions, including continuous visibility of the lunar far side and advantageous communication geometry. Nevertheless, these trajectories are inherently unstable and require periodic corrective maneuvers to counteract natural divergence. Thus, Station-Keeping (S/K) becomes an essential operational activity, directly affecting propellant consumption and mission lifetime.

A further critical challenge arises from eclipse events generated by the Earth and the Moon. Depending on injection conditions and orbital geometry, prolonged shadow periods may exceed the sustainable discharge capability of onboard batteries, potentially compromising mission continuity. Since injection epochs are often dictated by external launch constraints, eclipse occurrence cannot always be avoided through trajectory design alone.

The coexistence of dynamical instability and geometric shadow constraints motivates the development of maneuver design strategies that integrate operational requirements directly into the control formulation. Rather than treating the station-keeping and eclipse mitigation as independent problems, this work investigates whether corrective maneuvers can be shaped to address both objectives simultaneously.

1.1. Research Objective

The aim is to develop a control-oriented methodology capable of maintaining the spacecraft within acceptable dynamical bounds while actively mitigating the most critical shadow events. Particular attention is devoted into assessing the magnitude of these corrective maneuvers and understanding the compatibility with the stringent constraints of the CubeSat platform. The research question of the thesis is:

To what extent can eclipse avoidance constraints be integrated into station-keeping strategies for Quasi-Halo orbits to improve robustness and operational feasibility, while minimizing the impact on the ΔV budget?

To answer this question, a methodology is developed within a high-fidelity dynamical framework, enabling realistic modeling of the cislunar environment and consistent evaluation of both control performance and propellant consumption.

1.2. Case Study: LUMIO

The Lunar Meteoroid Impacts Observer (LUMIO) [5] spacecraft, represents a relevant testbed of this new generation of cislunar CubeSats. LUMIO is a 12U-XL ESA mission led by the DART Group at Politecnico di Milano, operating on a Quasi-Halo orbit around the Earth–Moon L_2 point, with the objective of observing meteoroid impact flashes on the lunar far side to improve the knowledge of the Lunar Meteoroid Environment. LUMIO will be launched as a secondary payload on a vehicle inserting a primary spacecraft onto a Weak Stability Boundary trajectory; consequently, its injection conditions are dictated by those of the main mission and eclipses events cannot be treated with a priori mission design.

2. Dynamical Models

The dynamical framework adopted for this work is designed to balance analytical insight and physical fidelity in the modeling of spacecraft motion in the cislunar environment.
The analysis begins with the Circular Restricted Three-Body Problem (CRTBP), which offers a simplified yet effective dynamical model of the Earth–Moon system. Within this framework, key dynamical features such as Libration points, periodic Halo orbits, and their intrinsic instability properties can be characterized. The CRTBP is used to generate an initial reference Halo orbit for the case study of the work, through a differential correction procedure.
However, due to the sensitivity of these trajectories to perturbations, a higher-fidelity representation is required to realistically assess long-term orbital behavior. For this reason, the Roto-Pulsating Restricted n-Body Problem (RPRnBP) is introduced, which accounts for additional gravitational perturbations, and solar radiation pressure providing a more accurate description of cislunar dynamics.
Following the procedure in [2], the periodic Halo orbit of the CRTBP is used as an initial guess and subsequently refined into a Quasi-Halo orbit, which is adopted as the reference trajectory for both station-keeping and eclipse avoidance investigations.

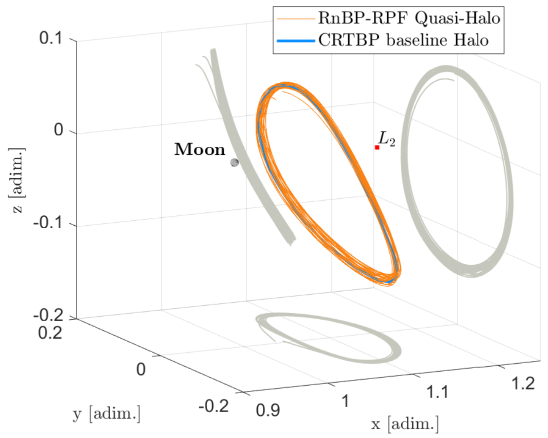

Figure 1: LUMIO Quasi-Halo orbit @ Earth–Moon Barycenter centered adimensional rotating frame.

3. Station-Keeping Techniques

For CubeSats equipped with chemical propulsion, impulsive correction strategies represent the most suitable solution for the station-keeping problem. Two principal families of techniques can be identified [4]. The first exploits the dynamical structure of the three-body problem, through the Floquet theory, by suppressing the unstable components of the motion along periodic trajectories. While theoretically effective, these approaches rely heavily on long-term State Transition Matrix propagation and may suffer from numerical limitations when applied in an high-fidelity environment and over mission-relevant time spans.
The second family includes targetig-based strategies, among which the Target Point Approach (TPA) has emerged as one of the most operationally viable solutions. TPA computes impulsive corrections by minimizing a weighted cost function involving position and velocity de-

viations from the reference trajectory. Due to its computational efficiency and proven reliability, it has been selected as the baseline station-keeping strategy for the LUMIO mission [5].
Eclipse mitigation can be addressed through either passive or active strategies. Passive approaches rely on trajectory design choices, such as selecting favorable injection epochs, exploiting synodic resonances, or refining periodic solutions with embedded eclipse constraints. These methods can yield naturally eclipse-free trajectories without additional propellant expenditure. However, they depend on narrow launch windows and precise phase control, and are often impractical when injection conditions are dictated by a primary payload.
Active strategies instead employ dedicated maneuvers to temporarily reshape the trajectory and avoid shadow regions. Existing approaches, such as multi-burn closed-loop procedures developed for Distant Retrograde Orbits [3], demonstrate feasibility but typically require optimization processes.

4. The LUMIO Mission

The operational framework adopted in this work reflects the actual mission assumptions defined for LUMIO. Station-keeping maneuvers are scheduled every 7 days, each preceded by a 2-day orbit determination cut-off. The control analysis accounts for realistic injection, navigation and maneuver execution errors, modeled according to mission specifications. A minimum impulse threshold of 5 mm/s is imposed, consistent with the spacecraft propulsion unit [5].
The nominal TPA is implemented and tested within a Monte Carlo framework to assess robustness under these operational uncertainties. The results show a mean annual station-keeping cost of 14.66 m/s, with a standard deviation of 1.97 m/s, a 3σ value of 20.96 m/s and no failures recorded.

4.1. Geometric Analysis

The geometric properties of the reference Quasi-Halo orbit are then analyzed to characterize eclipse occurrences and severity. Since eclipse timing and depth depend on the relative configuration between spacecraft, Earth, Moon and Sun, the trajectory is transformed into two dedicated rotating frames [3]:

- Earth-Centered Sun-Earth Rotating frame (ECSER);
- Moon-Centered Sun-Moon Rotating frame (MCSMR).

In these frames, the Sun-body direction is aligned with the x-axis, and the shadow cones generated by the primaries remain fixed in space. This representation simplifies eclipse detection and allows direct geometric interpretation of shadow penetration in a computationally efficient fashion. The Conical Shadow Model is adopted to compute both umbra and penumbra regions. This implementation is validated through the comparison with the SPICE[1] `gfoclt` function, confirming consistency in event timing and durations.
The analysis reveals that eclipses events are highly variable along the nominal orbit. Their severity is quantified through the depth of shadow penetration, which directly correlates with power subsystem stress. Once the injection epoch is fixed, these events are structurally embedded in the orbit geometry. For the considered reference trajectory, the eclipse events detected are shown in Fig. 2.

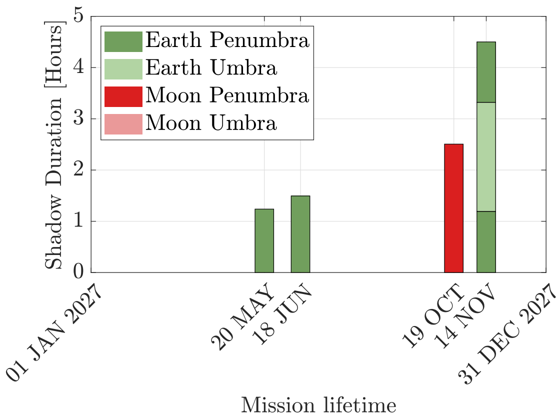

Figure 2: Lighting condition of LUMIO Quasi-Halo reference trajectory.

5. Methodology

In this section, the formulated deterministic, constraint-based station-keeping strategy with active eclipse avoidance for Quasi-Halo orbits is presented. Instead of relying on global trajectory optimization (often sensitive to initial guesses and computationally heavy), this approach builds a local, analytically tractable pro-

[1] `https://naif.jpl.nasa.gov/naif/toolkit.html`

cedure based on Karush-Khun-Tucker (KKT) conditions [1].
A general optimization problem is formulated as $\min_{\boldsymbol{x}} F(\boldsymbol{x})$, subject to the m constraints and the simple bounds, respectively:

$$\boldsymbol{c}_L \leq \boldsymbol{c}(\boldsymbol{x}) \leq \boldsymbol{c}_U,\ \boldsymbol{x}_L \leq \boldsymbol{x} \leq \boldsymbol{x}_U. \tag{1}$$

The KKT necessary conditions require feasibility, stationarity of the Lagrangian $\mathcal{L}(\boldsymbol{x}, \boldsymbol{\lambda}) = F(\boldsymbol{x}) - \boldsymbol{\lambda}^T \boldsymbol{c}(\boldsymbol{x})$, and satisfaction of complementary slackness conditions [1]. Linearizig the optimality system via Newton's method leads to the classical KKT linear system:

$$\begin{bmatrix} \boldsymbol{H}_{\mathcal{L}} & -\boldsymbol{G}^T \\ \boldsymbol{G} & \boldsymbol{0} \end{bmatrix} \begin{bmatrix} \Delta\boldsymbol{x} \\ \Delta\boldsymbol{\lambda} \end{bmatrix} = \begin{bmatrix} -\boldsymbol{g} \\ -\boldsymbol{c} \end{bmatrix}. \tag{2}$$

Where $\boldsymbol{H}_{\mathcal{L}}$ is the Hessian of the Lagrangian, $\boldsymbol{G}$ the Jacobian of the constraints, and $\boldsymbol{g}$ the gradient of the objective function. This formulation is equivalent to solving a quadratic-linear subproblem [1]:

$$\mathcal{F}(\boldsymbol{x}) = \boldsymbol{g}^T \Delta\boldsymbol{x} + \frac{1}{2} \Delta\boldsymbol{x}^T \boldsymbol{H}_{\mathcal{L}} \Delta\boldsymbol{x}, \tag{3}$$

subject to the linear constraints $\boldsymbol{G}\Delta\boldsymbol{x} = -\boldsymbol{c}$.

5.1. Eclipse Avoidance Formulation

A continuous shadow function $g(\boldsymbol{x}, t)$ provides a signed measure of the spacecraft's proximity to the shadow boundary: $g > 0$ means sunlit and $g < 0$ means eclipse penetration. A safety margin g_{safe} is introduced to limit eclipse depth according to battery discharge capability, expressed from the empiric formula given by the manufacturer:

$$42[W]t_{\text{pen}}[h] + 71[W]t_{\text{umb}}[h] < 86.8[Wh]. \tag{4}$$

The eclipse constraint is then written as $g(\boldsymbol{x}_e, t_e) \geq g_{\text{safe}}$, where the subscript "e" represents the deepest eclipse point.
Eclipse avoidance is implemented locally as a two-impulse control problem. Since eclipse events are fully determined once the injection epoch and the corresponding reference trajectory are defined, all relevant quantities (such as the deepest eclipse epoch, the reference STMs, and the shadow function outputs) can be computed a priori. The decision variable is then:

$$\boldsymbol{z} = \left[\Delta\boldsymbol{v}_1^T, \Delta\boldsymbol{v}_2^T\right]^T \quad \in \mathbb{R}^6. \tag{5}$$

The eclipse constraint defined is intrinsically non-linear. Thus, to exploit it within the KKT framework, it must be linearized about the reference state at the enforcement epoch. Using STM-based propagation and the control vector $\boldsymbol{z}$, the deviation from the nominal orbit is:

$$\begin{aligned} \delta\boldsymbol{x}(t) =& \boldsymbol{\Phi}(t_{m,1}, t)\delta\boldsymbol{x}_{m,1}^- + \dots \\ &+ \boldsymbol{\Phi}(t_{m,1}, t)G\Delta\boldsymbol{v}_1 + \dots \\ &+ \boldsymbol{\Phi}(t_{m,2}, t)G\Delta\boldsymbol{v}_2. \end{aligned} \tag{6}$$

The shadow constraint is linearized:

$$g(\boldsymbol{x}_e, t_e) \approx g_0 + \nabla\boldsymbol{g}_e^T \delta\boldsymbol{x}(t_e) \geq g_{\text{safe}}, \tag{7}$$

where $\nabla\boldsymbol{g}_e$ is the gradient of the shadow function, computed with finite differences. After some mathematical manipulation, the constraint can be written in a compact form as:

$$\boldsymbol{a}^T\boldsymbol{z} \geq \psi. \tag{8}$$

The objective function combines soft stationkeeping, minimizing the deviation at a future target point (12 days), together with the minimization of the cost of the maneuver:

$$J_{\text{avoid}}(\boldsymbol{z}) = J_{S/K}(\boldsymbol{z}) + J_c(\boldsymbol{z}). \tag{9}$$

Combining the two definitions, stacking the terms yields the quadratic form:

$$\begin{aligned} \min_{\boldsymbol{z}\in\mathbb{R}^6} \quad & \boldsymbol{z}^T\boldsymbol{H}\boldsymbol{z} - 2\boldsymbol{f}^T\boldsymbol{z} \\ \text{with} \quad & \begin{cases} \boldsymbol{H} := \boldsymbol{A}_{qp}^T\boldsymbol{A}_{qp}, \\ \boldsymbol{f} := \boldsymbol{A}_{qp}^T\boldsymbol{b}_{qp}, \end{cases} \\ \text{such that} \quad & \boldsymbol{a}^T\boldsymbol{z} \geq \psi \end{aligned} \tag{10}$$

Introducing the Lagrange multiplier, μ, defined further below, the KKT system is:

$$\begin{bmatrix} 2\boldsymbol{H} & -\boldsymbol{a} \\ \boldsymbol{a}^T & 0 \end{bmatrix} \begin{bmatrix} \boldsymbol{z} \\ \mu \end{bmatrix} = \begin{bmatrix} 2\boldsymbol{f} \\ \psi \end{bmatrix}. \tag{11}$$

If the constraint is satisfied, the unconstrained solution is found as $\boldsymbol{z}_{a,0} = \boldsymbol{H}^{-1}\boldsymbol{f}$. Otherwise, the constrained solution will be:

$$\boldsymbol{z}_{a,1} = \boldsymbol{H}^{-1}\boldsymbol{f} + \frac{1}{2}\mu\boldsymbol{H}\boldsymbol{a} \tag{12}$$

The value of μ is obtained by enforcing the feasibility condition:

$$\mu = \frac{2\left(\psi - \boldsymbol{a}^T\boldsymbol{H}^{-1}\boldsymbol{f}\right)}{\boldsymbol{a}^T\boldsymbol{H}^{-1}\boldsymbol{a}} \tag{13}$$

The two burns are applied respectively 12 and 6 days before the deepest eclipse epoch. Nominal TPA maneuvers are suspended in the 14 days preceding the eclipse to allow effective deviation from the reference trajectory.

5.2. Recovery Nominal Orbit Formulation

After the avoidance phase, trajectory deviations increase due to the intrinsic instability of the orbit, requiring recovery maneuvers to bring the spacecraft back inside the predefined linearity tube where the linearized dynamics remain valid. This mathematical construct provides a statistical characterization of the maximum allowable deviation from the reference trajectory at a certain epoch for which the linearized dynamics remain a valid approximation, thus ensuring proper functioning of subsequent TPA corrections. The linearity tube constraint is defined as:

$$\left\|\delta \boldsymbol{r}(t^*)\right\| \leq \rho(t^*). \tag{14}$$

This is written as a nonconvex constraint, hence, to preserve analytical tractability within the KKT framework, it is projected on the direction of the unconstrained expansion of the flow $\hat{\boldsymbol{n}}$. Considering the same control vector of Eq. (5), the linearization of the position deviation similarly as in Eq. (6) and projecting along $\hat{\boldsymbol{n}}$, the linearized constraint in a compact form is:

$$\boldsymbol{b}^T \boldsymbol{z} \leq \beta. \tag{15}$$

The objective function for the recovery maneuvers is defined in the same way as the avoidance ones. The problem in the least-squared formulation is:

$$\begin{aligned} \min_{\boldsymbol{z}\in\mathbb{R}^6} \quad & \boldsymbol{z}^T \boldsymbol{W} \boldsymbol{z} - 2\boldsymbol{p}^T \boldsymbol{z} \\ \text{with} \quad & \begin{cases} \boldsymbol{W} := \boldsymbol{A}_{qp}^T \boldsymbol{A}_{qp}, \\ \boldsymbol{p} := \boldsymbol{A}_{qp}^T \boldsymbol{b}_{qp}, \end{cases} \\ \text{such that} \quad & \boldsymbol{b}^T \boldsymbol{z} \leq \beta. \end{aligned} \tag{16}$$

Introducing the Lagrange multiplier ν, the KKT system is:

$$\begin{bmatrix} 2\boldsymbol{W} & \boldsymbol{b} \\ \boldsymbol{b}^T & 0 \end{bmatrix} \begin{bmatrix} \boldsymbol{z} \\ \nu \end{bmatrix} = \begin{bmatrix} 2\boldsymbol{p} \\ \beta \end{bmatrix}. \tag{17}$$

The unconstrained solution is computed as $\boldsymbol{z}_{r,0} = \boldsymbol{W}^{-1}\boldsymbol{p}$ if the tube constraint is already satisfied. Alternatively, the constrained solution will be:

$$\boldsymbol{z}_{r,1} = \boldsymbol{W}^{-1}\boldsymbol{p} - \frac{1}{2}\nu \boldsymbol{W}^{-1}\boldsymbol{b}. \tag{18}$$

The value of ν is obtained enforcing the feasibility condition:

$$\nu = \frac{2\left(\boldsymbol{b}^T \boldsymbol{W}^{-1}\boldsymbol{p} - \beta\right)}{\boldsymbol{b}^T \boldsymbol{W}^{-1}\boldsymbol{b}}. \tag{19}$$

The first recovery burn is applied at the deepest eclipse epoch, followed by a second burn 2 days later. A second two-burn sequence is executed, as numerical simulations highlighted that two burns are not enough to fully recovery the nominal orbit. Nominal TPA is suspended for 8 days after the eclipse and then restarted.

6. Results

The proposed methodology is tested through numerical simulations for different possible reference Quasi-Halo orbits (three test cases) for the LUMIO mission. The analysis evaluates the effectiveness of the proposed methodology in terms of eclipse mitigation capability, control of trajectory deviations, and ΔV expenditure. Figure 3 presents the time history of the corrective maneuvers: nominal TPA corrections remain small outside eclipse seasons, while avoidance and recovery burns produce localized $\|\Delta \boldsymbol{v}\|$ peaks during eclipse intervals. The largest control effort occurs for the last event, whose long and deep eclipse induces significant trajectory deviations requiring stronger recovery actions.

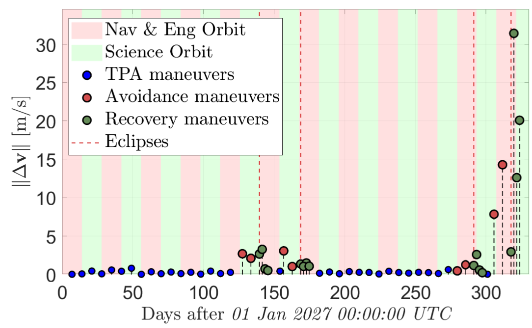

Figure 3: $\Delta \boldsymbol{v}$ magnitude of the maneuvers.

Figure 4 shows that early eclipses are significantly shortened or avoided, while the longest event is mitigated sufficiently to remain within the imposed power threshold.

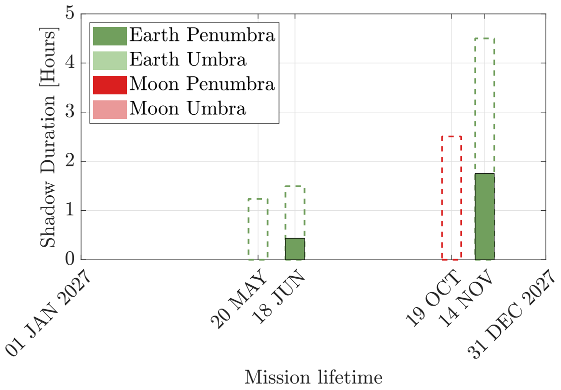

Figure 4: Lighting condition of LUMIO simulated trajectory.

The results confirm effective eclipse mitigation, with deviations of several thousand kilometers explaining the magnitude of the required avoidance and recovery maneuvers.

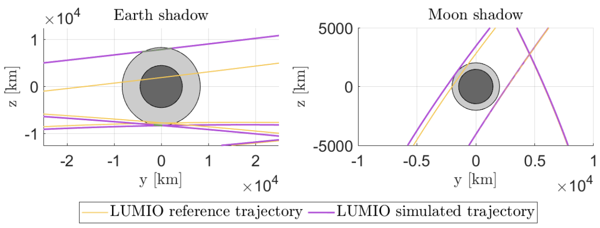

Figure 5: Close-up views @ ECSER (right) and @ MCSMR (left).

The control effort is dominated by the most critical eclipse event. Nominal station-keeping remains low ($\Delta v_{S/K} = 8.4116$ m/s), while the total cost $\Delta V_{tot} = \Delta v_{avoid} + \Delta v_{recovery} + \Delta v_{S/K} = 126.4539$ m/s exceeds the nominal budget. This value should be interpreted as a conservative upper bound resulting from the robust containment strategy adopted in the analysis.
Test Case 2, characterized by a single Moon eclipse, requires a significantly lower control effort ($\Delta V_{tot} = 30.9009$ m/s), achieving complete eclipse avoidance with a reduced ΔV compared to Test Case 1. Test Case 3 represents an intermediate scenario, where both lunar and terrestrial eclipses are mitigated while maintaining operational feasibility and bounded state deviations ($\Delta V_{tot} = 39.9989$ m/s). The Monte Carlo analysis of 1000 samples per case confirms limited dispersion of ΔV_{tot} and an almost negligible failure rate, demonstrating the robustness of the proposed strategy under realistic uncertainties.

7. Conclusions

The numerical results demonstrate that the proposed active eclipse avoidance and recovery strategy is effective and robust within the adopted high-fidelity dynamical framework. Eclipse events are successfully mitigated while maintaining bounded trajectory deviations and compatibility with nominal station-keeping. In particular, Moon eclipses and short Earth eclipses can be avoided with a manageable ΔV expenditure, confirming the practical applicability of the method.
However, long and deep Earth eclipses require great trajectory deviations, leading to propellant costs that may exceed the available budget. In such worst-case conditions, the methodology remains dynamically robust but becomes demanding from a fuel standpoint. Monte Carlo analyses confirm limited dispersion of the total ΔV and an almost negligible failure rate, supporting the statistical reliability of the approach.
Overall, the developed technique provides a viable and transferable framework for active eclipse mitigation in CubeSat missions operating in cislunar environments, with its feasibility ultimately governed by eclipse severity and associated propellant constraints.

References

[1] J. T. Betts. *Practical Methods for Optimal Control and Estimation Using Nonlinear Programming*. SIAM, 2010.

[2] D. A. Dei Tos and F. Topputo. Trajectory refinement of three-body orbits in the real solar system model. *Advances in Space Research*, 2017.

[3] Y. Shang, C. Wen, Y. Sun, H. Zhang, and Y. Gao. Active solar eclipse avoidance on the distant retrograde orbit of the earth–moon system. *Advances in Space Research*, 2024.

[4] M. Shirobokov, S. Trofimov, and M. Ovchinnikov. Survey of station-keeping techniques for libration point orbits. *Journal of Guidance, Control, and Dynamics*, 2017.

[5] F. Topputo, C. Giordano, A. Martinelli, C. Buonagura, G. Merisio, F. Piccolo, A. Rizza, and P. Panicucci. LUMIO Phase B Mission Analysis Report (MAR). 2023.